Trapping of an Activated HF Molecule inside a Double Four-Ring Unit: A Quantum Chemical Model of the Microporous Fluorinated Gallium Phosphate ULM-18

Francis Taulelle,[†] Josep-M. Poblet,*[,‡] Gérard Férey,[§] and Marc Bénard*[,||]

Contribution from the RMN et Chimie du Solide, UMR 7510 ULP-Bruker-CNRS, Université Louis Pasteur, 4 rue Blaise Pascal, 67070 Strasbourg Cedex, France, Departament de Química Física, Universitat Rovira i Virgili, Pç Imperial Tarraco, 43005 Tarragona, Spain, IREM, UMR 173, Université de Versailles-Saint Quentin, 45 Avenue des Etats-Unis, 78035 Versailles Cedex, France, and Laboratoire de Chimie Quantique, UMR 7551 ULP-CNRS, Université Louis Pasteur, 4 rue Blaise Pascal, 67070 Strasbourg Cedex, France

Received June 21, 2000. Revised Manuscript Received October 19, 2000

Abstract: The penetration of a proton into the prenucleation building unit of a microporous gallophosphate and its interaction with an encapsulated fluorine anion have been investigated by means of DFT calculations. The inorganic part of the fluorinated gallophosphate ULM-18 has been modeled by a neutral, double four-ring (D4R) unit of formula $[(GaOH)_4(HPO_4)_4 \cdot H_2O]$ encapsulating the fluorine ion. Assuming the cage to be rigid and to retain throughout the calculations the geometry determined from X-ray diffraction (XRD), the position of F^- has been optimized, either as an isolated guest species or in the presence of an incoming proton. In agreement with the XRD structure, the fluorine atom has been shown to occupy in both cases a nonsymmetric position in the cage, being attached to three gallium atoms out of four. The distribution of the molecular electrostatic potential inside and outside the $(F^-)@[(GaOH)_4(HPO_4)_4 \cdot H_2O]$ system has provided indications concerning the pathways that could be used by an incoming proton to penetrate the D4R unit and to approach the fluorine anion. The migration of a proton from an external site of fixation to the interior of the D4R unit has been found possible through two faces out of six. In both cases, the process has been found exothermic by ∼0.17 eV and the energy barrier was estimated to ∼0.8 eV. Inside the gallophosphate cage, the proton first adopts a position typical of a strong F···H···O bond made possible through an important shift of the fluorine anion away from the tripod of bonded gallium atoms. Then, the $F^- \cdots H^+$ system can easily evolve back and forth on a flat potential curve beetween one of the F···H···O bonded conformations and a situation characterized by the cleavage of the H···O link and the formation of a moderately activated F−H molecule, with the fluorine still attached to three gallium atoms.

1. Introduction

The hydrothermal synthesis of microporous material can be viewed as the templated aggregation process of prenucleation building units (PNBUs) that are assumed to exist as independent fragments before the formation of the crystalline phase.[1,2] It has been recently recognized that some rearrangement may occur between the structure of the PNBUs and that of the building units of the crystalline compound.[3,4] Those rearrangements explain the multiplicity of the crystal structures obtained from the same starting material, depending on the experimental conditions. They are therefore characteristic of the topological organization during nucleation and crystal growth. The fluorinated gallophosphate ULM-18 has been recently synthesized and characterized by X-ray diffraction (XRD) and NMR.[5] This material consists of macroanionic layers of formula $[Ga_4(PO_4)_5HF]^{3-}$ intercalated with $[(CH_3)_2NHCH_2CH_2NH(CH_3)_2]^{2+}$ and H_2O. The inorganic sheet is composed of double-four ring (D4R) units that are linked together by an isolated phosphate group located at a corner of each cuboidal cage (Figure 1). The X-ray structure confirmed that the fluorine atom occupies a templating position inside each D4R unit as in ULM-5,[2] octadecasil,[6] cloverite,[7] and other fluorinated zeolite-like material.[8] At variance with cloverite I and octadecasil, however, the position of the fluorine atom is strongly off-center and preferentially linked to three gallium atoms.[5] The last fluorine-to-gallium distance (3.157 Å) is much too long to consider a possible Ga−F bond, and the coordination sphere of this latter gallium atom, composed of five oxygens, is not compatible with such a bond (Figure 2). Moreover, ^{19}F NMR and $^{31}P-\{^1H\}$ cross-polarization magic angle spinning (CPMAS) spectra indicate that the proton needed for charge compensation of the

[†] RMN et Chimie du Solide, Université Louis Pasteur.
[‡] Universitat Rovira i Virgili.
[§] Université de Versailles-Saint Quentin.
[||] Laboratoire de Chimie Quantique, Université Louis Pasteur.

(1) Breck, D. W. *Zeolite, Molecular Sieve, Structure Chemistry and Use*; Wiley-Interscience: New York, 1974.
(2) Férey, G. *J. Fluorine Chem.* **1995**, *72*, 187.
(3) Taulelle, F.; Haouas, M.; Gérardin, C.; Estournès, C.; Loiseau, T.; Férey, G. *Colloids Surf. A* **1999**, *158*, 299.
(4) Taulelle, F.; Pruski, M.; Amoureux, J.-P.; Lang, D.; Bailly, A.; Huguenard, C.; Haouas, M.; Gérardin, C.; Loiseau, T.; Férey, G. *J. Am. Chem. Soc.* **1999**, *121*, 12148.
(5) Taulelle, F.; Samoson, A.; Loiseau, T.; Férey, G. *J. Phys. Chem. B* **1998**, *102*, 8588.
(6) Caullet, P.; Guth, J. L.; Hazm, J.; Lamblin, J. M.; Gies, H. *Eur. J. Solid State Inorg. Chem.* **1991**, *28*, 345.
(7) Estermann, M.; McCusker, L. B.; Baerlocher, C.; Merrouche, A.; Kessler, H. *Nature* **1991**, *352*, 320.

10.1021/ja0022167 CCC: $20.00
Published on Web 12/14/2000

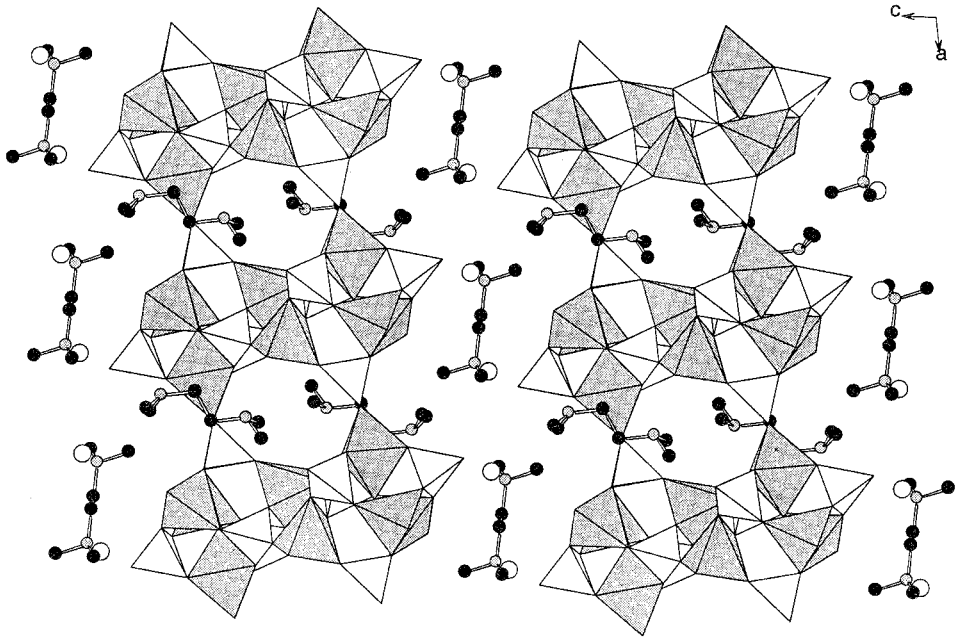

Figure 1. Projection of the structure of ULM-18 near [010]. Open circles indicate water molecules. Hydrogen atoms of the organic template are omitted for clarity.

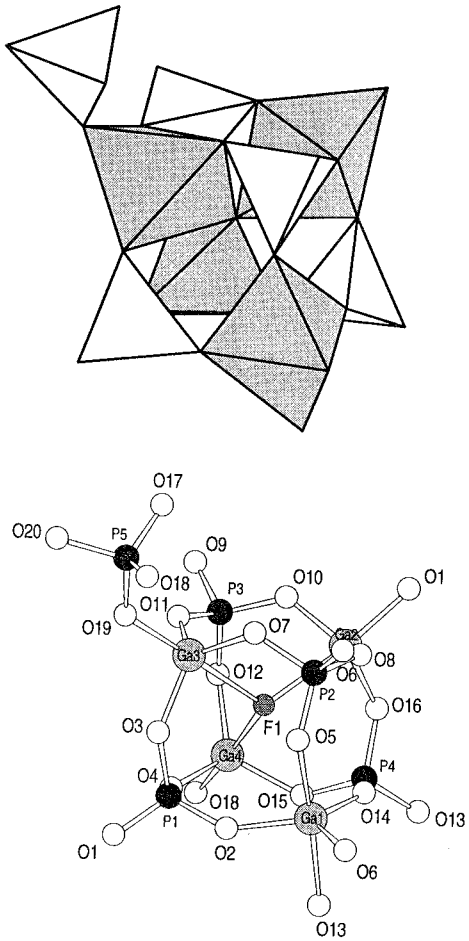

Figure 2. Polyhedral and atomic representations of the asymmetric unit, from X-ray determination.

network should also be located inside the D4R unit.[5] The composite shape of the NMR signal suggests that this insider hydrogen could occupy at least three distinct positions in the cage, but the nature of the coupling between the proton and the fluorine atom was not firmly established. Is the encapsulated proton either strongly acidic and mobile or covalently linked to the fluorine atom? Is it susceptible to strolling in and out across the walls of the D4R unit? Better knowledge concerning these points could shed some light on the nucleation mechanism and on the nature of the templating agent, either F^- or HF. In case of a condensation mechanism involving fluorine anions, the possibility for proton diffusion through the faces of the preformed building units should be established to account for charge compensation. We intend to address those questions by investigating, by means of DFT calculations, the preferred positions of a fluorine anion confined with a proton inside a model of the D4R unit.

2. Model and Methods

The model used throughout the project was that of an isolated cage composed of four PO_4 tetrahedra, three GaO_4F trigonal bipyramids, and one GaO_5 trigonal bipyramid, representing one D4R unit. This cage structure, completed with an encapsulated proton, was made electrically neutral by hydroxylating eight terminal oxygens out of nine. The last terminal oxygen, bonded to Ga(1) with a long Ga−O distance of 2.004 Å, was assumed to be part of a coordinated water molecule. The approach that consists of terminating cluster models of infinite lattices with OH or H in order to ensure electroneutrality and remove dangling bonds has been successfully adopted in various recent studies mimicking zeolites or SiO_2 surfaces or glasses.[9] However, attempts to optimize the geometry of the proposed gallophosphate cage showed that the

(8) (a) Simmen, A.; Patarin, J.; Baerlocher, C. *9th International Zeolite Conference* **1993**, *1*, 433. (b) Kallus, S.; Patarin, J.; Marler, B. *Microporous Mater.* **1996**, *7*, 89. (c) Reinert, P.; Patarin, J.; Loiseau, T.; Férey, G.; Kessler, H. *Microporous Mesoporous Mater.* **1998**, *22*, 43. (d) Schott-Darie, C.; Patarin, J.; Le Goff, P. Y.; Kessler, H.; Benazzi, E. *Microporous Mater.* **1994**, *3*, 123. (e) Schreyeck, L.; Caullet, P.; Mougenel, J.-C.; Patarin, J.; Paillaud, J.-L. *Microporous Mesoporous Mater.* **1997**, *11*, 161. (f) Feng, P. Y.; Bu, X. H.; Stucky, G. D. *Nature* **1997**, *388*, 735. (g) Reinert, P.; Schott-Darie, C.; Patarin, J. *Microporous Mesoporous Mater.* **1997**, *9*, 107. (h) Reinert, P.; Marler, B.; Patarin, J. *J. Chem. Soc., Chem. Commun.* **1998**, 1770. (i) Loiseau, T.; Férey, G. *J. Solid State Chem.* **1994**, *111*, 407. (j) Loiseau, T.; Férey, G. *J. Mater. Chem.* **1996**, *6*, 1073. (k) Serpaggi, F.; Loiseau, T.; Férey, G. *J. Chem. Soc., Chem. Commun.* **1997**, 1093. (l) Férey, G. *C. R. Acad. Sci. Ser. C* **1998**, *1*, 1. (m) DeBord, J. R. D.; Reif, W. M.; Warren, C. J.; Haushalter, R. C.; Zubieta, J. *Chem. Mater.* **1994**, *9*, 1194. (n) Lii, K.-H. *J. Porous Mater.* **1998**, *5*, 147. (o) Riou, D.; Taulelle, F.; Férey, G. *Inorg. Chem.* **1996**, *35*, 6392. (p) Wragg, D. S.; Hix, G. B.; Morris, R. E. *J. Am. Chem. Soc.* **1998**, *120*, 6822.

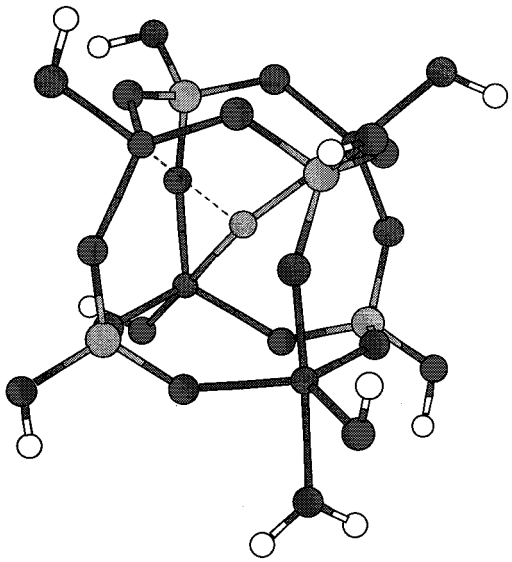

Figure 3. XMOL representation of the $F^-@[(GaOH)_4(HPO_4)_4{\cdot}H_2O]$ cage molecule used to model the D4R inorganic unit: dark gray circles, O and Ga; light gray circles, P and F; white circles, H. The broken line represents the F−Ga(3) bond (2.41 Å, Table 1).

model structure is exceedingly flexible and responds to the presence and to the displacement of an insider proton by wide range distortions. This quasi-fluxional character of an isolated D4R unit is reminiscent of the large flexibility that is expected from prenucleation building units.[4] It is not compatible, however, with the scope of the present study, which rather concerns the nucleation stage at which the molecular framework has already acquired a certain rigidity. The above-described model of the D4R unit was therefore assigned the geometry obtained from XRD and completed with standard values for the O−H distances. Those geometrical parameters were then kept fixed throughout the calculations, except for those defining the position of the encapsulated fluorine atom. The equilibrium position of the fluorine atom was optimized first for the unprotonated model system $F^-@[(GaOH)_4(HPO_4)_4{\cdot}H_2O]$ (Figure 3). The three Ga−F bond distances defining the nonsymmetric position of the fluorine anion in the cage are reproduced with reasonable accuracy (Table 1): Ga(2)−F = 2.249 Å (exp, 2.213 Å); Ga(4)−F = 2.259 Å (exp, 2.246 Å); Ga(3)−F = 2.431 Å (exp, 2.353 Å). The last, nonbonding, Ga···F distance was calculated to be 3.079 Å, compared to an XRD value of 3.16 Å.

The geometry optimizations have been carried out by means of the DFT formalism with gradient corrections for exchange and correlation, as implemented in the ADF program.[10] The formalism is based upon the local spin density approximation characterized by the electron gas exchange (Xα with $\alpha = {}^2/_3$) together with Vosko−Wilk−Nusair[11] parametrization for correlation. Nonlocal corrections due to Becke for the exchange energy[12] and to Perdew for the correlation energy[13] have been added. For oxygen, a 1s frozen core was described by means of a single Slater function. For the other non-hydrogen atoms, the frozen core composed of the 1s and 2sp shells for phosphorus, from the 1s to 3sp shells for gallium, was also modeled by a minimal Slater basis. For all atom types, the Slater basis set used for the valence shell is of triple-ζ quality and completed by a polarization function.[14] The geometry optimization processes have been carried out by minimizing the energy gradient by the BFGS formalism[15] combined with a DIIS-type convergence acceleration method.[16] The optimization cycles were continued until all of the three following convergence criteria were fulfilled: (i) the difference in the *total energy* between two successive cycles is less than 0.001 hartree; (iii) the difference in the *norm of the gradient* between two successive cycles is less than 0.01 hartree. $Å^{-1}$; (iii) the maximal difference in the *Cartesian coordinates* between two successive cycles is less than 0.01 Å.

The regions to be investigated preferentially for the proton localization inside the D4R unit and for defining its diffusion pathway through selected faces of the cube were characterized after a topological analysis of the molecular electrostatic potential (MEP) distribution[17] generated by the $F^-@[(GaOH)_4(HPO_4)_4{\cdot}H_2O]$ model and obtained from Hartree−Fock calculations. These calculations were carried out by means of the Asterix program[18] using all-electron basis sets of triple-ζ quality on the valence shells. The choice of Hartree−Fock to derive MEP distributions was justified by the study of Luque et al, concluding that the MEP determined from the SCF wave function remains largely unaffected by correlation effects in regions located outside the van der Waals sphere.[19] After the study had been completed, we however derived from the DFT density representations of the MEP in the six planes of Figure 4. These representations are provided as Supporting Information and show that the topology of the MEP distribution and the relative depths of the MEP minimums obtained at the Hartree−Fock level are adequately reproduced by the DFT calculations.

3. Results and Discussion

3.1. The Calculated Protonation Sites. MEP maps have been derived for the anionic model $F^-@[(GaOH)_4(HPO_4)_4{\cdot}H_2O]$ in all planes defined by the fluorine atom and by a pair of doubly

(9) (a) Lopez, N.; Illas, F.; Pacchioni, G. *J. Phys. Chem. B* **1999**, *103*, 1712, 8552. (b) Lopez, N.; Illas, F.; Pacchioni, G. *J. Am. Chem. Soc.* **1999**, *121*, 813. (c) Civalleri, B.; Barrone, E.; Ugliengo, P. *Chem. Phys. Lett.* **1998**, *294*, 103. (d) Kessi, A.; Delley, B. *Int. J. Quantum Chem.* **1998**, *68*, 135. (e) Uchino, T.; Yoko, T. *J. Chem. Phys.* **1998**, *108*, 8130. (f) Corma, A.; García, H.; Sastre, G.; Viruela, P. M. *J. Phys. Chem. B* **1997**, *101*, 1712, 4575. (g) Xu, T.; Kob, N.; Drago, R. S.; Nicholas, J. B.; Haw, J. F. *J. Am. Chem. Soc.* **1997**, *119*, 12231.

(10) (a) *ADF 2.3 User's Guide*; Chemistry department: Vrije Universiteit, Amsterdam, The Netherlands, 1997. (b) Baerends, E. J.; Ellis, D. E.; Ros, P. *Chem. Phys.* **1973**, *2*, 41. (c) te Velde, G.; Baerends, E. J. *J. Comput. Phys.* **1992**, *99*, 84. (d) Fonseca-Guerra, C.; Visser, O.; Snijders, J. G.; te Velde, G.; Baerends, E. J. *Methods and Techniques in Computational Chemistry: METECC-95*; Clementi, E., Corongiu, G., Eds.; STEF: Cagliari, Italy, 1995; pp 305−395.

(11) Vosko, S. H.; Wilk, L.; Nusair, M. *Can. J. Phys.* **1980**, *58*, 1200.

(12) (a) Becke, A. D. *J. Chem. Phys.* **1986**, *84*, 4524. (b) Becke, A. D. *Phys. Rev.* **1988,** *A38*, 3098.

(13) Perdew, J. P. *Phys. Rev.* **1986**, *B33*, 8882; **1986**, *B34*, 7406. To calibrate the results obtained with the Becke−Perdew (BP86) functional, the binding energies calculated for some protonation sites of Table 1 were recomputed using the same basis sets and another gradient corrected functional, known as Perdew−Wang 91 (PW91: Perdew, J. P.; Wang, Y. In *Electronic Structure of Solids 1991*; Ziesche, P., Eschrig, H., Eds.; Akad. Verlag Berlin: Berlin, 1991) also available with the ADF package. The results are as follows: O(5)a int, −221.204 eV; O(14) int, −220.669 eV; O(2) int, −220.507 eV. The binding energies are therefore uniformly shifted by ∼4.0 eV with respect to BP86, but the energy *differences* between the various protonation sites are modified by less than 0.01 eV. Since the Perdew−Wang functionals have been shown to give a fair account of van der Waals interactions in weakly bound systems (see: Lorenzo, S.; Lewis, G. R.; Dance, I. *New J. Chem.* **2000**, *24*, 295. Wesolowski, T. A.; Ellinger, Y.; Weber, J. *J. Chem. Phys.* **1998**, *108*, 6078), it probably means that induction and dispersion forces are not major actors in the determination of the proton equilibrium position.

(14) Snijders, J. G.; Baerends, E. J.; Vernooijs, P. *At. Nucl. Tables* **1982**, *26*, 483. (b) Vernooijs, P.; Snijders, J. G.; Baerends, E. J. *Slater type basis functions for the whole periodic system*; Internal Report, Free University of Amsterdam, The Netherlands, 1981.

(15) Fisher, T. H.; Almlöf, J. *J. Phys. Chem.* **1992**, *96*, 9768.

(16) Versluis, L. Ph.D. Thesis, University of Calgary, Calgary, Alberta, Canada, 1989.

(17) The MEP is a local property defined as the energy of a positive unit charge undergoing at a given point of space the charge distribution of an unperturbed, neighboring molecule. In the atomic unit system, it is expressed in $e{\cdot}(b)^{-1}$ (when considered as a potential) or in hartrees (1 hartree = 27.2 eV) when applied to a real proton and considered as an energy. The *electric field* derived from the potential is expressed either in atomic units, or in $e{\cdot}Å^{-2}$, with $1\ e{\cdot}Å^{-2} = 0.28\ e{\cdot}(b)^{-2}$. See: *Molecular Electrostatic Potentials, Concepts and Applications*; Murray, J. S., Sen, K., Eds.; Elsevier: Amsterdam, 1996. And more specifically the contribution by: Vetrivel, R.; Deka, R. C.; Chatterjee, A.; Kubo, M.; Broclawik, E.; Miyamoto, A. on pp 509−541 for applications to microporous materials.

(18) (a) Ernenwein, R.; Rohmer, M.-M.; Bénard, M. *Comput. Phys. Chem.* **1990**, *58*, 305. (b) Rohmer, M.-M.; Demuynck, J.; Bénard, M.; Wiest, R.; Bachmann, C.; Henriet, C.; Ernenwein, R. *Comput. Phys. Chem.* **1990**, *60*, 127.

(19) Luque, F. J.; Orozco, M.; Illas, F.; Rubio, J. *J. Am. Chem. Soc.* **1991**, *113*, 5203.

Table 1. Binding Energies (BE, eV) with Respect to a Collection of Neutral Atoms, Calculated for the Protonated Form of a Model of ULM-18 Made of the Rigid and Electrically Neutral Gallophosphate Cage $[(GaOH)_4(HPO_4)_4 \cdot H_2O]$ (referred to as D4R), Encapsulating a Fluoride Ion[a]

system	protonation site	BE (eV)	protonation energy (eV)	relative BE[b]	*d*(F−Ga) (Å) Ga(2)	Ga(3)	Ga(4)	Δ*P*(F)[c] (Å)	*d*(F−H) (Å)	*d*(O−H) (Å)	∠(OHF) (deg)
protonated (F^-@D4R)											
exp					2.21	2.35	2.25	0			
calc	O(10) ext	−217.286	−10.98	0	2.178	2.353	2.252	0.05			
	O(16) ext	−217.174	−10.87	0.112	2.187	2.388	2.234	0.04			
	O(5) ext	−217.033	−10.73	0.253	2.254	2.315	2.451	0.28			
	O(8) ext	−216.794	−10.49	0.492	2.198	2.342	2.254	0.06			
	O(12) ext	−216.699	−10.39	0.587	2.229	2.342	2.267	0.035			
	O(11) ext	−216.579	−10.27	0.707	2.212	2.294	2.255	0.09			
	O(14) ext	−216.456	−10.16	0.830	2.187	2.551	2.301	0.29			
	O(3) ext	−215.980	−9.67	1.306	2.168	2.392	2.257	0.05			
	O(5)a int	−217.201	−10.89	0.085	2.407	2.453	2.364	0.43	1.034	1.417	172
	O(5)b int	−217.156	−10.85	0.130	2.370	2.374	2.330	0.30	1.001	1.560	164
	O(5)c int.	−216.982	−10.68	0.304	2.270	2.421	2.292	0.20	0.975	1.740	150
	O(14) int	−216.657	−10.35	0.629	2.167	2.641	2.318	0.39	1.018	1.484	174
	O(2) int	−216.503	−10.20	0.783	2.24	2.36	2.24	0.04	0.95	2.18	160
(F^-@D4R)		−218.886			2.227	2.412	2.225	0.08			
D4R		−210.020									
F^-		−4.14									

[a] Each protonation site is defined by the proximal oxygen and is either "external" (outside the cage) or "internal" (inside the cage). The Ga−F distances and, for the internal protonation sites, the geometrical parameters of the strong F···H···O hydrogen bond are indicated. The electron affinity of fluorine and binding energies calculated for D4R and for F^-@D4R are also given. [b] The relative binding energies are identical to the relative protonation energies. [c] Deviation with respect to the experimental position.

bridging oxygen atoms opposite on the same cubic face. The vicinity of several electronegative atoms is expected to generate basins of low potential susceptible to attract an incoming proton. Six of those maps are displayed in Figure 4. A large number of MEP minimums—corresponding to nucleophilic regions—are observed in every plane. Most of those minimums, and the deepest ones, are located on the outer side of the D4R unit. This should not appear surprising: previous studies on polyoxometalate hosts have shown that the convex side of a metal oxide surface is basic, whereas the concave side is acidic.[20,21] In the present case, the situation is made slightly more complex by the presence of the guest anion, the fluorine atom, considered as an integrated part of the system and expecting the incoming of another guest, the proton. The MEP distribution displays a deep potential minimum (-0.23 e·Å^{-1}) in the vicinity of the fluorine atom and opposite to the tripod formed by the three Ga−F bonds (Figure 5). This region of low potential extends toward the three bridging oxygens coordinated to Ga(1), namely, O(2, 5, 14) (see Figure 3). The MEP maps of Figure 4 show that channels of low potential, representing a priori favorable pathways to the approach and to the fixation of an incoming proton do exist between (i) F and O(2), (ii) F and O(5), and (iii) F and O(14) and nowhere else. The MEP distribution around O(5) and to a lesser extent, around O(2) and O(14), appears markedly different from that of the other bridging oxygens of the D4R unit: when most bridging oxygens display a deep MEP minimum oriented *outside* the cage, no such minimum is observed around O(5), but rather a large valley of low potential starting near the surface of the D4R unit and extending *inside* the cage (see Figure 4). This MEP distribution seems to mark oxygen O(5) out as a pivotal atom making the inner part of the cage accessible to the proton and determining its pathway(s) toward the eventual protonation sites.

The binding energies associated with several sites of protonation, either external or internal to the D4R unit, are collected in Table 1, together with the corresponding position of the fluorine atom, defined by the four F−Ga distances. For each considered protonation site, the deviation Δ*P*(F) of the calculated fluorine position with respect to the XRD determination is given. The sequence of protonation energies obtained with the present model, however, suggests that the internal protonation sites are quite competitive with the external ones. The most stabilizing position obtained for H^+ is the external site facing O(10) (protonation energy: −10.98 eV);[22] but the circulation pathway of the proton around O(5) and across the gallophosphate cage is marked out with low-energy positions outside the cage (−10.73 eV) but also inside (−10.68 to −10.89 eV, Table 1). This represents a correction to the indications obtained from the electrostatic potential distribution, which predicted external protonation to be largely favored. Other external sites with relatively large protonation energies were also characterized in the vicinity of several doubly bridged oxygen atoms belonging to the cubic framework (Table 1). As noticed above, the external protonation sites characterized in the vicinity of O(5) and O(14), both coordinated to Ga(1), could rather be termed "facial", since the position of the attached proton is located just above a face of the D4R unit defined by the average plane of four bridging oxygens. The proton fixation is slightly less exothermic on those "facial" sites (−10.73 eV near O(5); −10.16 eV near O(14)) than on the most favored external sites O(10) and O(16). More important and significant, however, is the fact that the "facial" fixation of the proton on O(5) or O(14) is also less exothermic than a migration through the walls of the D4R unit to reach the

(20) Rohmer, M.-M.; Devémy, J.; Wiest, R.; Bénard, M. *J. Am. Chem. Soc.* **1996**, *118*, 13007.

(21) Rohmer, M.-M.; Bénard, M.; Blaudeau, J.-P.; Maestre, J.-M.; Poblet, J.-M. *Coord. Chem. Rev.* **1998**, *178−180*, 1019.

(22) Since the binding energy (BE) of either a molecule or an ion is defined with respect to the energy of a collection of isolated, *neutral* atoms, the protonation energy (PE) at protonation site X of the fluorinated D4R unit is calculated as: $PE_{(site\ X)}[F^-@D4R] = BE[H_{(site\ X)}\cdots F@D4R] - BE[F^-@D4R] - IE[H]$, where IE[H] is the ionization energy calculated for the hydrogen atom, i.e., 12.65 eV. The protonation energy at site O(10) is therefore equal to $-217.286 + 218.96 - 12.65 = -10.976$ eV (Table 1). If this protonation energy is assumed to be zero, the *relative* protonation energies calculated at the other sites reproduce the sequence of the relative binding energies given in Table 1. In a similar way, the protonation energy of F^- is equal to $BE[HF] - E[F^-] - IE[H]$, where $E(F^-)$ is the calculated electron affinity of F, −4.14 eV. This gives $-7.95 + 4.14 - 12.65 = 16.46$ eV.

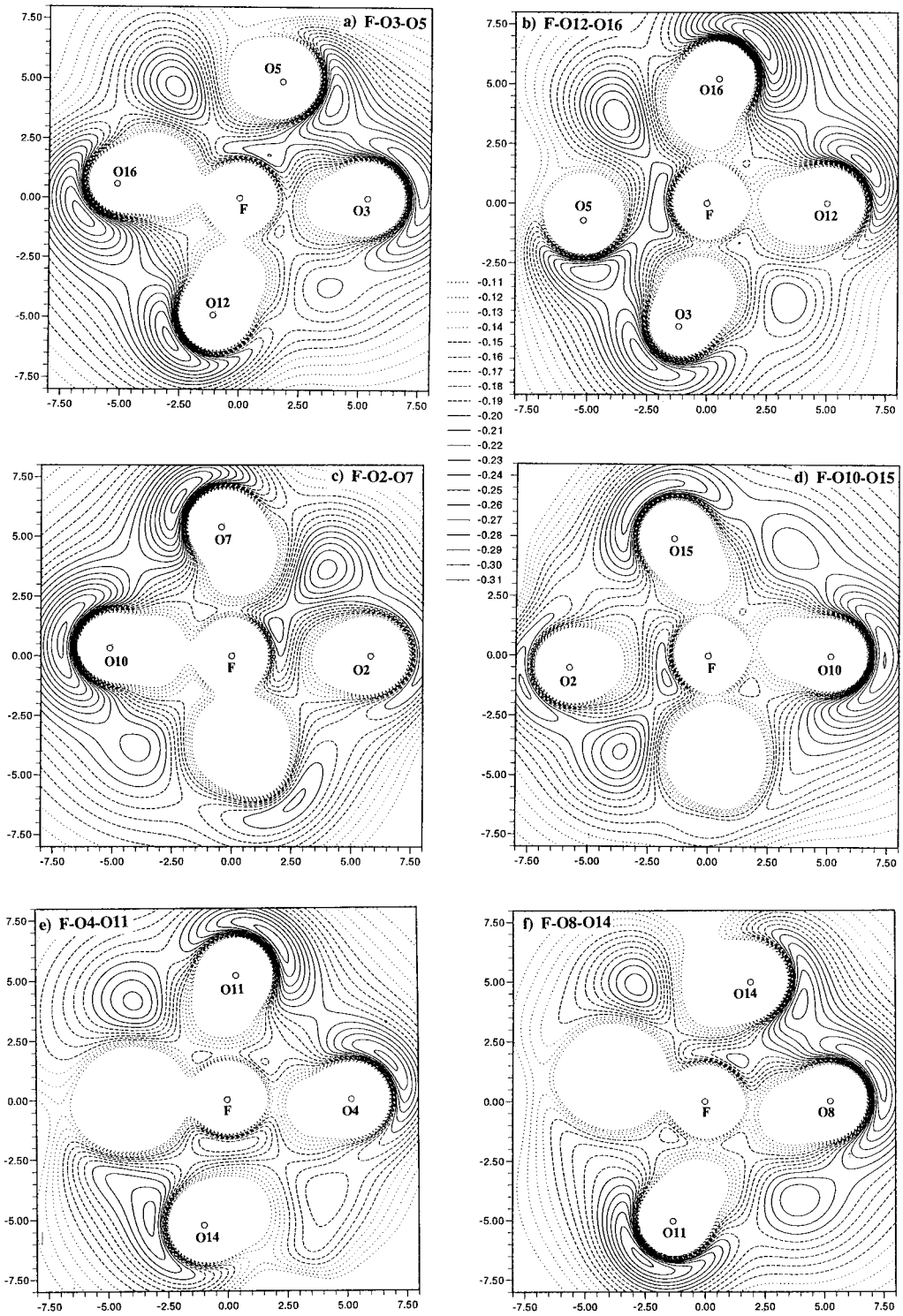

Figure 4. Electrostatic potential maps (MEP, atomic units[17]) computed in six planes each containing the fluorine anion and two oxygen atoms occupying opposite positions on a face of the D4R unit: (a) plane F O(3) O(5); (b) plane F O(12) O(16); (c) plane F O(2) O(7); (d) plane F O(4) O(11); (e) plane F O(8) O(14); (f) plane F O(10) O(15). Distances in bohrs (1 bohr = 0.5292 Å); contour interval, 0.01 au.

proximal inner protonation site. The "facial" protonation sites could therefore be considered as initial positions in penetration pathways allowing the proton to cross the D4R unit.

Several internal protonation sites have been characterized (Table 1). It appears, however, that the potential energy surfaces relating the fluorine atom, the internal proton, and at least one oxygen atom of the cage are extremely flat and floppy. Some sites characterized as local minimums, especially in the vicinity of O(5) could rather correspond to intermediate positions in a fluxional process affecting the F···H system. However, all positions of the F···H moiety characterized as internal protonation sites (Table 1) can each be associated with one of the low-potential channels connecting F to O(2), O(5), and O(14), respectively. Some of those conformations are displayed in Figure 6. The sequence of the protonation energies can be correlated with the MEP values obtained across the channels and in the vicinity of the fluorine atom (Figure 4). The inner site, which appears most favored according to the criterion of the protonation energy, is almost exactly lying on the F···O(5) line ($\angle$FHO = 172°). The calculated protonation energy is

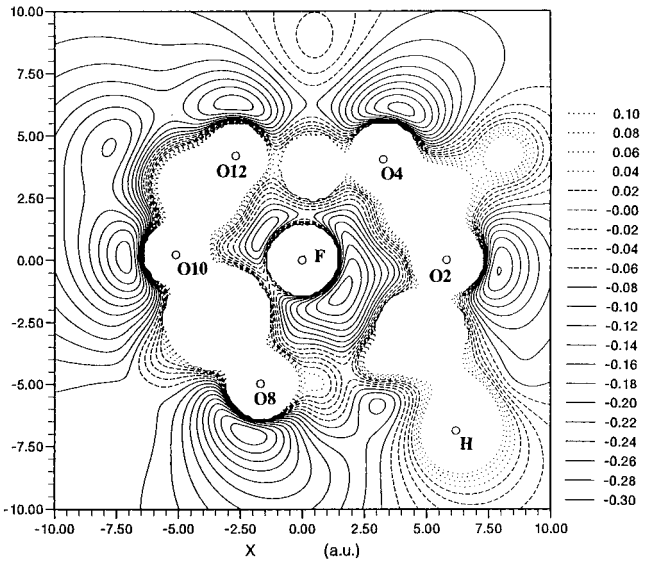

Figure 5. MEP map in the plane defined by F, O(2), and O(4). Contour interval, 0.02 au.

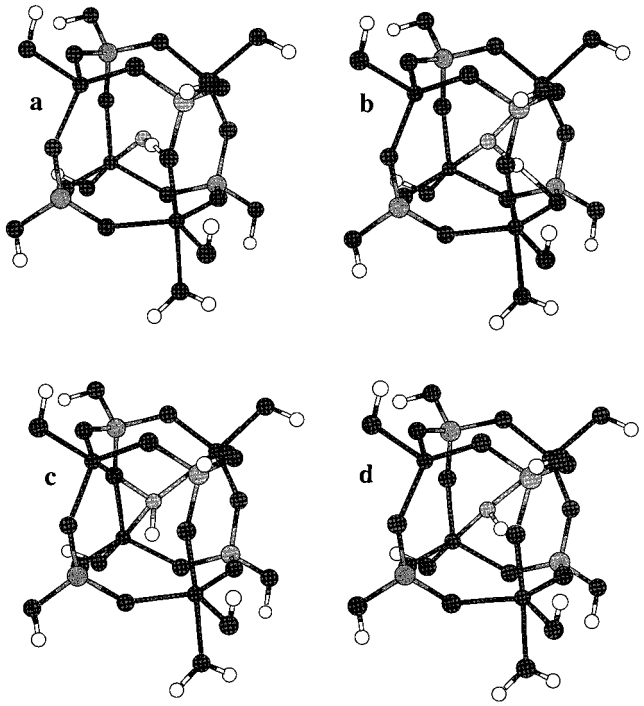

Figure 6. XMOL representation of four conformations with low energy for internal protonation: (a) O(5)···H···F conformation; (b) O(14)···H···F conformation; (c) F−H conformation (H pointing toward O(2)); (d) F−H conformation (H pointing toward O(5)).

−10.89 eV, which is only 0.09 eV higher than for the best external site. The F−H distance, 1.034 Å, corresponds to an important activation of the F−H bond: the F−H distance calculated in an isolated molecule is 0.935 Å. The distance between the proton and O(5) is 1.417 Å, characteristic of a strong interaction without covalent bond formation. In fact, these structural parameters are reminiscent of some geometrical arrangements calculated or observed for systems displaying very strong hydrogen bonds.[23] In linear, centered difluoride ions, the observed H···F distance is close to 1.135 Å.[23,24] Ab initio calculations on carboxylic acid−fluoride associations indicated that by assuming O, H, and F collinear, the optimal geometry for the R−COO···H−F system corresponds to $d_{O\cdots H} = 1.38$ (R═H) or 1.40 Å (R = Me) and to $d_{H-F} = 0.99$ Å.[23,25]

Particularly stable conformations with the proton inside the D4R unit are associated with protonation energies of −10.68, −10.35, and −10.20 eV, higher by 0.21−0.79 eV than for the site near O(5) (Table 1). In one of these sites, the geometrical arrangement of the proton between F and O(14) can also be interpreted in terms of an important activation of the H−F molecule (Table 1).

The nature of two other protonation sites characterized by the calculations and referred to as O(2) and O(5)c (Table 1, Figure 6) seems to be different. An activation of the F−H bond is still perceptible: at 0.95 Å for the O(2) site and 0.975 Å for the O(5)c site, the F−H distance remains sensibly stretched. At variance with the former sites, these arrangements of the protonated species do not display the geometrical characteristics of strong F···H···O hydrogen bonds. In the O(2) site, the F, H, and O(2) atoms are not far from being collinear (∠FHO = 160°), but the O···H distance remains quite large, 2.18 Å. No sensible displacement of the fluorine atom in the direction of O(2) is evidenced from the calculations (Table 1). The absence of a strong hydrogen bond conformation connecting F to O(2) could be correlated with the position calculated for the F^- ion assumed encapsulated alone in the D4R unit: the distance between F and O(2) (3.08 Å) is appreciably longer than either between F and O(5) (2.76 Å) or between F and O(14) (2.81 Å). The formation of a strong F···H···O hydrogen bond involving O(2) is therefore a priori more demanding than the same type of bond involving O(5) or O(14). In the O(5)c protonation site, the fluorine atom has experienced a migration with respect to its optimal position in the unprotonated cage, but this transfer is not oriented toward a specific oxygen; the stretching of all three Ga−F bonds rather suggests a weakening of the link with the tripod of gallium atoms. Interestingly, another equilibrium position O(5)b was characterized for the proton approximately midway between the strong hydrogen bond conformation O(5)a and the moderately activated F−H bond described in protonation site O(5)c. The associated energy is only 0.04 eV higher than for O(5)a (Table 1). Those results suggest that a delicate balance might exist between two topologies, both possible for the Ga_3−F−H moiety. One bonding mode can be described as a rather strong F−H link ($d_{F-H} < 1$ Å) with no specific interaction with any of the surrounding oxygen atoms. Quite at variance with this description is the alternate bonding mode, which implies an elongated F···H bond ($d_{F-H} > 1$ Å), a link with an oxygen atom characteristic of a strong F···H···O interaction, and an important elongation (>0.2 Å) of the F−Ga bond which is approximately trans to the F···H···O bond.

Both bonding types could be characterized from the calculations with the proton evolving in the vicinity of O(5) (sites referred to as O(5)a and O(5)c, Table 1, Figure 6a,d). It is clear from Table 1 that, *within the framework of the present model*, the F···H···O(5) hydrogen bond is thermodynamically favored. However, the average position of the fluorine atom observed from XRD in ULM-18 rather suggests that the opposite energy ordering prevails in the real system (see section 3.3). Considering now the proton oriented either toward O(2) or toward O(14), a single bonding mode only could be characterized. No strong hydrogen bond was found between F and O(2). As noted above, this should be assigned to the relatively long F···O(2) distance, which requires an important and energetically expensive displacement of F to generate the three-center interaction. The

(23) Emsley, J. *Chem. Soc. Rev.* **1980**, 91.
(24) Ibers, J. A. *J. Chem. Phys.* **1964**, *40*, 402.
(25) Emsley, J.; Hoyte, O. P. A.; Overill, R. E. *J. Chem. Soc. Perkin Trans. 2* **1977**, 2079.

protonation site characterized along this orientation can therefore be simply described as a moderately activated F−H bond (d_{F-H} = 0.95 Å). The opposite situation prevails for the protonation site located between O and F(14): the hydrogen-bonded conformation only could be characterized.

3.2. Energetics of the Protonation in the D4R Unit. Some remarks can be made about the protonation energy values obtained either for the external or for the internal protonation sites. First, the electrostatic attraction experienced by the proton undergoing the molecular field at the protonation site represents only a fraction of the protonation energy, and this fraction changes according to the nature of the protonation site, either external or internal. The electrostatic energy at the two preferred external protonation sites (O10 and O16) is of the order of −0.30 hartree, that is −8.15 eV. This represents ∼75% of the calculated proton energy, and the rest should be assigned to covalent bonding. As calculated and displayed in Figure 4, the MEP minimums inside the cage are noticeably higher than outside and close to the surface. However, the penalty resulting from an accommodation of the proton in the vicinity of the fluorine anion does not exceed a few kilocalories per mole, and this should be attributed to an important increase, from 25 to ∼45%, of the proportion of covalent bond energy. An immediate, and partly correct, interpretation of this increase results from a correlation with the covalent bond energies observed for the OH radical (−4.64 eV)[26] and for the FH molecule (−6.11 [26] or −5.87 eV[27]). The covalent bond energy is indeed stronger for FH, but the bonding conditions and the associated energetics inside the D4R unit are rather far from those yielding an isolated, covalently bound FH molecule. Let us first consider the calculated bonding energy corresponding to the reaction $F^- + H^+ \rightarrow FH$, −16.46 eV,[22] of which about −10 eV is of electrostatic origin. The protonation energy calculated for the encapsulated fluoride ion is much lower, −10.89 eV only, when the proton occupies the most favorable internal site, including −6.0 eV (−0.22 hartree, see Figure 4) ascribed to the electrostatic attraction. A large part of the energy difference with respect to the reaction of the free ion pair is however regained from the bond energy between F^- and the D4R unit, −4.73 eV (Table 1). In that sense, the energetics of the internal protonation confirm the analysis made above from purely geometrical considerations: the activation of the HF molecule occurring in the gallophosphate cage can be viewed as initiated by the Ga−F bond tripod, which reduces both the net charge on fluorine (−0.42 e) and the propensity to give a strong covalent bond with the incoming proton. The bond activation may then be enhanced by an attractive interaction induced by the closest oxygen neighbor.

3.3. Where is the Proton in ULM-18? The composite line shape obtained for the ^{19}F NMR signal in ULM-18 has been interpreted as evidence for the presence of hydrogen localized in various positions inside the D4R.[5] This should not be interpreted as contradictory, with the present results indicating the energetically preferred protonation site to be located on the external side of the model cage. First, the difference between the protonation energies calculated for the best *external* and for the preferred *internal* sites remains remarkably small, about 0.09 eV, despite the difference in the associated electrostatic potentials being more than 1 order of magnitude larger. Furthermore, the present model is limited to the inorganic part of the system; in the real crystal structure, a network of strong hydrogen bonds has been evidenced among the terminal oxygens of the $[Ga_4(PO_4)_5HF]^{3-}$ framework, the water molecule, and the tetramethylethylenediamine dications.[5] Even though the bridging oxygens are not directly taking part in that network, the close vicinity of the cationic moieties is expected to significantly raise the relative values of the external MEP minimums.

Less evident to interpret appear the displacements of the fluorine atom in the cage in response to the proton fixation (Table 1). It has been mentioned already that the position optimized for the fluorine anion, assumed to be the sole guest atom in the cage, correctly reproduces the XRD determination: the calculated position of F is distant by only 0.08 Å from the experimental one. The fluorine ion has been displaced toward the center of the cage, which corresponds to an average stretching of 0.035 Å for the three Ga−F bonds (Table 1). Let us now consider the influence of an incoming proton. In the two positions that have been assimilated to strong F−H···O hydrogen bonds, the proton drags the fluorine ion further away from the tripod of bonded gallium atoms, to approach either O(5) or O(14) (Figure 6a,b). In the first case, the Ga(2)−F bond (2.407 Å) is elongated by 0.20 Å with respect to the XRD geometry, and a significant stretching (∼0.10 Å) is also obtained for the other two Ga−F bonds. The other F···H···O conformation induces an elongation of the Ga(3)−F bond by 0.29 Å. It is clear that those conformations cannot correspond to the most populated protonation sites of ULM-18, even though the F···H···O(5) conformation is energetically favored within the framework of the rigid, isolated D4R unit model. Since the interpretation of the ^{19}F NMR signal is not compatible with a fixation of the proton on the external side of the cage, then only the two internal sites, associated with short, moderately activated F−H bonds can be reasonable candidates for the conformation most populated in the real system. The position optimized for fluorine and the three Ga−F bond lengths in both conformations are in reasonable agreement with the XRD results (Table 1). A minor contribution from the conformations with strong F···H···O bonds is not at all excluded, however. In fact, the small energy differences calculated along the migration pathway followed by the proton in the vicinity of O(5) (conformations O(5)a,b,c in Table 1) suggest that the behavior of the proton could be fluxional along the valleys of low potential surrounding O(5), O(14), and the fluorine anion itself. Such a movement of the proton between F−H-like and F···H···O-like conformations would be concerted with an important scrambling of the fluorine anion.

3.4. Proton Migration. It has been shown in the previous section that H^+ and F^- encapsulated in the D4R unit can hardly be described as occupying one or several fixed positions, but rather behave as fluxional partners oscillating between the formation of a hydrogen bond with either O(5) or O(14) and the breaking of any specific link with oxygen to give a moderately activated HF molecule. This description accounts for the composite shape of the ^{19}F NMR spectrum, since three different pathways, following the valleys of low internal MEP can be characterized for the fluxional displacement of the proton: (i) from O(5) to F, (ii) from O(14) to F, and (iii) around F. However, it does not settle the mobility problems raised by the presence of a proton encapsulated in the D4R unit together with the fluorine anion: (i) Does this proton exhibit a detectable acidity, or in other words, what is its propensity to diffuse *out* of the cage? (ii) What is the nature of the templating agent, either HF or F^-, given that the latter possibility implies the

(26) Pople, J. A.; Frisch, M. J.; Luke, B. T.; Binkley, J. S. *Int. J. Quantum Chem., Symp.* **1983**, *17*, 307.

(27) Radzig, A. A.; Smirnov, B. M. *Reference Data on Atoms, Molecules, and Ions*; Toennies, J. P., Ed.; Springer Series in Chemical Physics; Springer-Verlag: Berlin, 1985, Vol. 31.

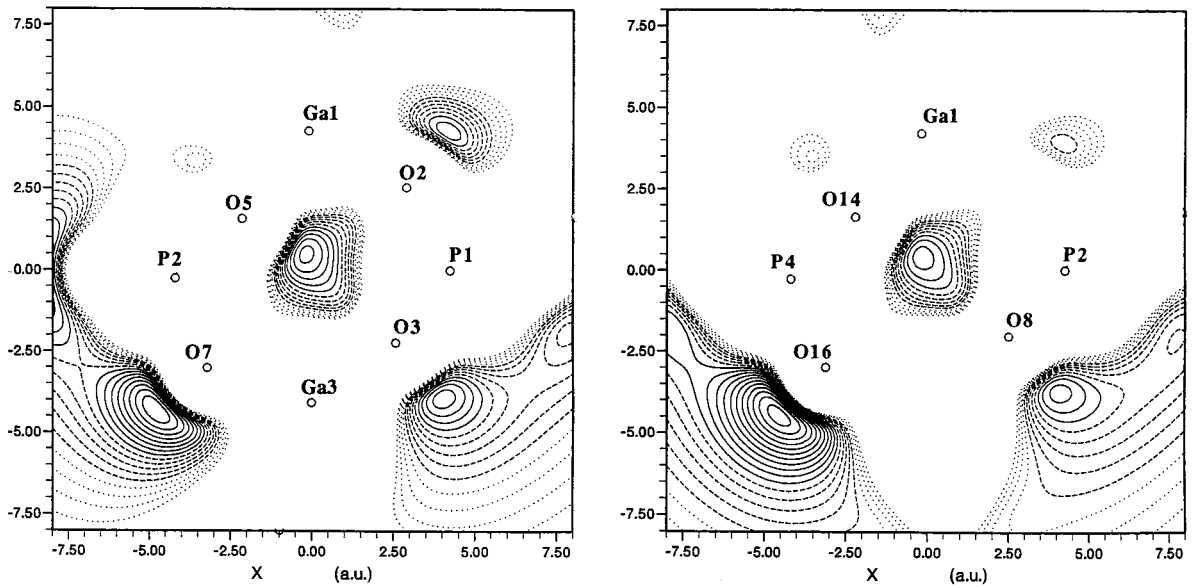

Figure 7. MEP maps calculated in the vicinity of the planes defining face 1 (average plane of O(2), O(3), O(5), O(7)) and face 2 (average plane of O(5), O(8), O(14). O(16)). Distances and contours as in Figure 4.

Table 2. Binding Energies (eV) Calculated for the Protonated Form of a F^-@D4R Model System[a]

position of the plane (Å)	face 1			face 2		
	energy (eV)	*d*(F−H) (Å)	*d*[O(5)−H] (Å)	energy (eV)	*d*(F−H) (Å)	*d*[O(14)−H] (Å)
1.0[b]	−217.033	3.121	1.004			
0.6[b]				−216.456	2.522	1.074
0.2	−216.446	2.148	1.279	−215.763	2.183	1.199
0.0	−216.366	1.932	1.292	−215.798	1.989	1.185
−0.2	−216.266	1.704	1.340	−215.657	1.803	1.159
−0.4	−216.276	1.404	1.457	−215.691	1.534	1.343
−0.6	−216.419	1.250	1.561	−215.899	1.298	1.524
−0.86[c]				−216.657	1.018	1.484
−0.99[c]	−217.201	1.034	1.417			

[a]pathways are characterized for the proton to cross the D4R cage either through face 1, represented as the average plane of the four oxygen atoms O(2, 3, 5, 7), or face 2, represented as the average plane defined by O(5, 8, 14, 16). A series of planes, parallel to face 1 and to face 2 and separated from each other by 0.2 Å, has been considered. The optimal positions of the proton in each of these planes, characterized by the associated binding energies, and by the distances to the fluorine ion and to the nearest oxygen atom, define the crossing pathways. [b] External minimum. [c] Internal minimum.

aptitude for the proton to move *inside* the preformed cage and get trapped therein? An answer to either question is conditioned by the possibility for the proton to cross, in or out, the walls of the inorganic layers. As for the problem of the proton location, the MEP distribution through the faces of the D4R unit could provide an indication about the feasability of the proton transfer and a guideline toward the definition of a migration channel. Figure 7 displays the MEPs in average planes defined from the XRD positions of oxygens O(2, 3, 5, 7) and O(5, 8, 14, 16) and referred to as face 1 and face 2, respectively. Those maps suggest that relatively small, but actual windows could exist for proton migration. Those windows are not symmetric with respect to the four oxygens of the face; the most electronegative regions are shifted toward O(5) for face 1 and toward O(14) for face 2. The existence of such windows could also be inferred from a careful examination of Figure 4, for example, by following the potential distribution along a line joining either O(3) to O(5) (Figure 4a) or O(2) to O(7) (Figure 4c) for face 1 and either O(8) to O(14) (Figure 4f) or O(5) to O(16) (Figure 4b) for face 2. The same figures also display the channels of low potential connecting those windows to the areas of proton scrambling defined above. The six maps of Figure 4 also confirm that no such channel does exist toward the other faces of the D4R unit. Furthermore, the "windows" of potential that open on these other faces all correspond to much higher MEP values. The definition of an energy pathway for a proton crossing the D4R unit has therefore been limited to face 1 and face 2.

A series of parallel planes, each separated by 0.2 Å, has been considered above and below the average plane of the four oxygen atoms defining a face of the cubic framework. The position of the proton in each plane has been optimized, under the same conditions as in the previous section: the cage framework is kept rigid, but the fluorine atom is free to move. The position of the proton with respect to fluorine and either O(5) for face 1 or O(14) for face 2 is defined in Table 2 for every plane, together with its associated energy. The sequence of the optimal proton positions in the series of equidistant parallel planes defines the pathway followed by the proton to cross the surface of the gallophosphate framework. To enter the cage, the proton starts from the local energy minimum associated with the facial protonation of O(5), on face 1, of O(14), on face 2 (Tables 1 and 2). Those local minimums are located about 1.0 and 0.6 Å above the average plane of the oxygen atoms, respectively (Table 2). An energy barrier is encountered, and the proton then makes its way down to what appears to be one of the internal protonation sites described as a strong F···H···O hydrogen bond. The last section of this pathway, corresponding to the formation of the F···H bond, is characterized by a important shift of the fluorine ion toward the proton. From there, as discussed above, the calculated energy

profile suggests a fluxional behavior of the proton between the conformation characteristic of the F···H···O linkage and a bonding situation where the proton is more specifically attached to fluorine. Another important point to notice is that, on both pathways, the energy of the inner position of the proton is lower than that of the external (or "facial") protonation site, by ∼0.2 eV. The penetration of a preformed D4R unit by a proton, should it be allowed by the height of the energy barrier, would therefore correspond to a slightly exothermic process. This exothermicity will therefore tend to keep the proton trapped into the D4R unit.

In both pathways, the energy barrier culminates close to 0.2 Å from the average plane of the four oxygens, on the inside (Table 2). The energy at the top of the barrier is ∼0.8 eV higher than that of the external minimum, and the energy gap with respect to the F···H···O conformation is very close to 1 eV through either face (Table 2). Since the MEP gradient along the downhill slope does not exceed 0.25 eV (Figure 4), most of the energy gain should be ascribed to the formation of the H−F covalent bond. This H−F covalent interaction is achieved, not by an approach of the proton but through the important stretching of the F−Ga bonds discussed above (Table 1). This displacement of the fluorine allows the proton to circle around O(5), or O(14) and to establish the F···H···O contact without moving away from the oxygen atom: in the final stage of the F···H···O bond formation, the H···O distance is even slightly *decreasing* as the fluorine atom approaches the proton (Table 2). Due to the noticeable stretching of the H−F bond in the hydrogen-bonded configurations and to the electrostatic influence of the molecular environment, the energy required for the dissociation of this bond—the energy barrier to a migration of the proton through the D4R unit *from the inside*—remains less than or equal to 1 eV in both considered cases (Table 2). This bond energy appears very low compared to the strength calculated for an isolated HF molecule, either with respect to an ion pair (−16.46 eV) or even with respect to neutral atoms (−6.67 eV). It is sufficient however to keep the proton trapped most of the time into the D4R unit, thus ensuring the electrical stability necessary to the growth of the crystal network.

3.5. Other Aspects. The present study has been restricted to the simple—or simplistic—model of a proton undergoing the field generated by a fluorine anion encapsulated in gallophosphate cage assumed to be neutral. Several factors that might influence the position of the proton in the cage or its migration trajectory at the early stage of the crystal formation have not been considered and will be briefly mentioned here. It should be first acknowledged that the present study has been focused on the *equilibrium positions* of the ion pair F^-/H^+. That is the reason the "heavy" fluorine ion has been allowed to relax, when this relaxation should not be considered in a dynamical modeling of the proton-transfer pathway. Such a dynamical study of the proton migration process should however pay attention to the large amplitude vibrations of the Ga−F bonds, which could initiate the proton trapping. A study on the kinetic aspects of the proton transfer should also account for tunneling, which has been suggested by Bell and by others to be a general pathway for proton-transfer reactions.[28]

(28) (a) Bell, R. P. *The Tunnel Effect*, 2nd ed.; Chapman and Hall: London, 1980. (b) Caldin, E.; Gold, V. *Proton Transfer*; Chapman and Hall: London, 1975. For recent studies, see: (c) Kim, Y.; Kreevoy, M. M. *J. Am. Chem. Soc.* **1992**, *114*, 7116. (d) Braun, J.; Schwesinger, R.; Williams, P. G.; Moromoto, H.; Wemmer, D. E.; Limbach, H.-H. *J. Am. Chem. Soc.* **1996**, *118*, 11101. (e) Cordonnier, M.; Coudert, H. *J. Mol. Spectrosc.* **1996**, *178*, 59. (f) Mackenzie, K.; Howard, J. A. K.; Siedlecka, R.; Astin, K. B.; Gravett, E. C.; Wilson, C.; Cole, J.; Gregory, R. G.; Tomlins, A. S. *J. Chem. Soc., Perkin Trans. 2* **1996**, 1749.

Table 3. Electrostatic Potential (Atomic Units[17]) Generated by a Point Charge Model of the Lattice Framework (+1 on the Nitrogen Atoms of the Protonated Amines, −3 on the Fluorine Atom Encapsulated in the Neighboring D4R Units) in Eight Positions Located Inside the Central Gallophosphate Cage, at Mid-Distance between the Fluorine Atom and the Gallium and Phosphorus Apexes, and at the Fluorine Position

position	potential ($e \cdot b^{-1}$)	position	potential ($e \cdot b^{-1}$)
F	+0.157	(F−P1)/2	+0.162
(F−Ga1)/2	+0.105	(F−P2)/2	+0.108
(F−Ga2)/2	+0.187	(F−P3)/2	+0.311
(F−Ga3)/2	+0.205	(F−P4)/2	+0.118
(F−Ga4)/2	+0.207		

The effect of the crystal lattice represents another factor that could deeply influence the distribution of the electrostatic potential inside the D4R unit. An estimate of the potential generated by the organic template and by the neighboring building units has been obtained from a point charge model of the crystal lattice in which a charge of +1 was assigned to each protonated amine function and located on the nitrogen atom, whereas the −3 charge of each neighboring D4R unit was assumed to be entirely localized on the crystal position of the fluorine atom. Eight points were considered inside the D4R unit under scrutiny, corresponding to the mid-distance between the fluorine atom and each of the gallium and phosphorus apexes. Successive shells of unit cells were positioned around this central D4R unit and their contribution to the lattice potential, calculated according to the point charge model, was added until convergence was reached. In practice, four shells of unit cells were sufficient to stabilize the third decimal of the potential values. The positioning of the unit cells and the summation of the point charge contributions have been carried out by means of the ELECTROS program.[29] The calculated values are displayed in Table 3.[30] The most important conclusion emerging from this model is that the lattice potential is not constant inside the D4R unit. An electric field of ∼0.13 $e \cdot Å^{-2}$ is oriented collinear to the direction going from P3 (high potentials) to the center of the Ga1−P2−P4 triangle (low potentials). The crystal field is therefore *practically opposite to the dipolar field associated with the F−H molecule in the average orientation determined in the present study, only considering an isolated D4R unit.* This result can be interpreted in two ways. If the crystal field is just superimposed to the field generated by the model of the isolated gallophosphate cage, it will do nothing but increase the trend toward proton transfer and fixation as described above. It is, however, dubious (i) that proton transfer and fixation occur within the fully rigid framework of an achieved crystal structure and (ii) that the orientation of the crystal field happens just by chance to be opposite to the F−H dipole. We rather suggest that the orientation of the crystal field represents a response to the proton fixation eventually yielding further stabilization of the structure through the dipole−dipole interaction.

4. Conclusion and Summary

Prenucleation building units condense to form a solid. They undergo density fluctuations followed, for the successful nuclei, by crystal growth. In $AlPO_4$-CJ2 nucleation and growth mechanism, it has been shown that isomerization of the prenucleation

(29) Ghermani, N. E.; Bouhmaida, N.; Lecomte, C. *ELECTROS: computer program to calculate electrostatic properties from high-resolution X-ray diffraction.* Internal Report URA CNRS 809, Université Henri-Poincaré-Nancy I, 1992.

(30) Different distributions of point charges were considered. The values of the potential were shifted appreciably, but the order of magnitude and the orientation of the electric field remained unmodified.

building unit is a "clipping" process that slows down the fluctuations of the nucleus, leading to further crystal growth. In the case of negatively charged D4R units, two processes are needed to ensure the successful evolution of a nucleus into a crystallite. The first is probably an isomerization process affecting the internal Ga−F−Ga bridging bonds in order to match the constraints of the crystalline network conformation. The second is a charge compensation mechanism allowing infinite condensation without accumulating negative charge. If this could not be realized, the accumulation of negative charges would end into a limited condensation as with highly charged polyanions. The proton insertion inside the D4R unit may accomplish both processes in a single step. By entering the D4R unit, the proton achieves the charge compensation process and induces at the same time some modifications of the Ga−F distances inside the unit. The energy provided by the rearrangement of the unit and the integration of the prenucleation building unit into the network can therefore be matched properly. This study has shown that the principal requirement needed for such an incorporation of hydrogen for charge compensation inside the D4R unit is fulfilled, namely, the definition of transfer pathways for the proton to cross the D4R unit with an acceptable value for the activation energy (<1 eV). Investigations carried out to characterize the positions preferred by H^+ and F^-, both encapsulated into the D4R unit, have evidenced a great lability of the proton inside the cavity. The incoming proton occupies first an intermediate, hydrogen-bond-like position, inducing an important shift in the position of the fluorine anion. A scrambling process affecting both F^- and H^+ is then expected to occur between the F···H···O bond structure and a conformational space where the encapsulated species can be described as a moderately activated HF molecule. The location calculated for the fluorine atom in these latter conformations closely matches the average site characterized from XRD. The lability of the encapsulated species most probably represents the optimal response to the contradictory requirements of topological network constraints and of prenucleation building unit optimal conformation. It allows a sufficiently large conformational space to adapt both constraints dynamically during the growth and thermodynamically for structure stability. This isomerization/charge compensation phenomenon might very well be a general feature of condensation processes, though only one single realization has been under study in this contribution.

Acknowledgment. Funding is acknowledged from the GDR 1164 of CNRS, aimed at the study of some fundamental aspects of the solid formation of microporous compounds. Calculations have been carried out for part at the IDRIS center (CNRS, Orsay, France) and for part on the workstations of the Departament de Química Física, purchased with funds provided by the DGICYT of the Government of Spain and by the CIRIT of Generalitat of Catalunya (Grants PB980916-C02-02 and SGR95-426).

Supporting Information Available: Maps of the molecular electrostatic potential in the six planes of Figure 4 from DFT/BP86 calculations carried out with the ADF program, as described in section 2 (PDF). This material is available free of charge via the Internet at http://pubs.acs.org.

JA0022167